Article

Shock-Induced Mesoparticles and Turbulence Occurrence

Tatiana A. Khantuleva [1,*] and Yurii I. Meshcheryakov [2]

1 Physical Mechanics Department, St. Petersburg State University, 28 Universitetsky pr., 198504 St. Petersburg, Russia
2 Institute of Problems of Mechanical Engineering, Russian Academy of Science, 61 Bolshoy pr., 199178 St. Petersburg, Russia
* Correspondence: khan47@mail.ru

Abstract: The development of a new approach to describe turbulent motions in condensed matter on the basis of nonlocal modeling of highly non-equilibrium processes in open systems is performed in parallel with an experiment studying the mesostructure of dynamically deformed solids. The shock-induced mesostructure formation inside the propagating waveform registered in real time allows the transient stages of non-equilibrium processes to be qualitatively and quantitatively revealed. A new nonlocal approach, developed on the basis of the nonlocal and retarded transport equations obtained within the non-equilibrium statistical physics, is used to describe the occurrence of turbulence. Within the approach, the reason for the transition to turbulence is that the non-equilibrium spatiotemporal correlation function generates the dynamic structures in the form of finite-size clusters on the mesoscale, with almost identical values of macroscopic densities moving as almost solid particles that can interact and rotate. The fragmentation of spatiotemporal correlations upon impact forms the mesoparticles that move at different speeds and transfer mass, momentum and energy-like wave packets. The movements recorded simultaneously at two scale levels indicate the energy exchange between them. Its description required a redefinition of the concept of energy far from local thermodynamic equilibrium. The experimental results show that the irreversible part of the dynamic mesostructure remains frozen into material as a new defect.

Keywords: turbulence; non-equilibrium correlation; self-organization; mesoparticle; wave packet; shock-induced waveform

1. Introduction

Turbulence, self-organization, non-equilibrium transport, mesostructures and living, despite their apparent differences, are all phenomena that are in fact closely related to each other. They are united by the nature of their processes far from local equilibrium, which have not been fully understood until now. The fact is that all classical science was based on the concept of thermodynamic equilibrium; many concepts outside this notion lose their physical meaning [1]. The use of high-speed and fast-flowing processes in modern technology requires going beyond the concept of continuum mechanics. Experimental studies of such processes have shown that they are accompanied by the self-organization of the multiscale internal structure of the system, including the eddy-wave turbulent structure, energy exchange between different scale levels, delay, the formation of internal control through feedback between the structure, its evolution and the change in macroscopic properties of the system [2–12]. The problem of mathematically describing such processes related to the problem of turbulence remains the most important unsolved problem of modern physics. No such fundamental theory has been developed that could be used as a basis for describing all the listed phenomena. Therefore, developing theoretical approaches for their adequate modeling is the most important task of modern physics.

An important role for the development of new approaches was played by experimental studies on shock loading of solids, which made it possible to trace some features of such

non-equilibrium processes in real time [2–6]. It was found that as a result of the impact, the solid material is partially turbulized on a mesoscopic scale inside the traveling wave as a liquid and then solidifies with a new defective structure. Revealing the regularities of such a process led to a deeper understanding of non-equilibrium transient processes.

It is commonly known that under shock loading at pressures below the elastic limit, elastic waves propagate without changing their form; the process of their propagation is reversible and is not accompanied by mass transport. The medium behavior is entirely described by the elastic modules in the framework of the conventional medium model of the elastic solid. Lastly, under long-time intensive loading, any medium manifests hydrodynamic behavior. The transport processes become irreversible because of the energy dissipation into heat. At the intermediate stage, the medium shows both elastic and hydrodynamic behavior. For example, the shock loading of a solid beyond the elastic limit induces the so-called two-wave structure of the elastic-plastic wave. The waveform changes during its propagation through the matter; the mass transportation becomes irreversible. Elastic modules begin to depend on strain-rate, whereas viscosity and relaxation time are determined by the size and geometry of the system. Under these conditions, the medium constants become functionals of transport processes, whereas conventional models of elastic body and viscous liquid appear to be incorrect. Such transient processes are not described within continuum mechanics concepts. In transient processes, deformation cannot be correctly subdivided into elastic and plastic components and phase and group velocities cannot be properly defined for non-stationary waves.

Short-duration loading of moderate intensity can be attributed to the transient types of non-equilibrium processes [10–12]. Experiments show that the conventional opinion that much of cold deformation work is transformed into heat, in case of dynamic deformation, does not respond to reality [13]. The higher the strain-rate, the less dynamic plastic work is shown to be transferred into heat. The rest of the deformation energy is absorbed by the medium to create internal boundaries and stored in the material, giving rise to cracks, shear bands and other structural defects [14,15]. Under shock loading, the time interval during which the force is applied to the impact surface is so short that the induced pressure wave is immediately scattered by the discrete atomic structure of the solid material. The unique studies on shock loading of solids carried out in real time [2] made it possible to conclude that the impact creates an inhomogeneous field of velocities of mesoscopic particles of the medium. One part of the dynamic structures reversibly disappears after stress relaxation and the other remains frozen in the material in the form of new defect structures (group of dislocations, shear bands, rotations). These studies allow us to conclude that the character of the movement of these mesoparticles is similar to the movement of solid particles in a turbulent flow of a concentrated dispersed mixture.

The physical nature of the processes on the mesoscale during high-rate deformation was unclear. No modern experimental tools can provide a visualization of the mesoparticles' motion at the time intervals comparable to the impact time. The various types of defects observed in the material after loading do not allow their evolution to be traced during stress relaxation. Therefore, it is necessary to develop such a theoretical model that could describe the entire process, both of the mesoparticles formation during shock loading and their evolution after the force stops acting.

In Section 2, some results of the experimental research on shock loading of solid materials are presented. These studies have shown that, similarly to the laminar-turbulent transition in a liquid, the transition to turbulent motion of mesoparticles in a solid under high-speed loading occurs in a threshold manner when the impact velocity exceeds a certain critical value. In this case, there is an increase in the rotational modes of motion of mesoparticles and a sharp increase in the stress loss at the wave compression plateau.

In Section 3, we notice that turbulent motions occur in the medium state far from local thermodynamic equilibrium that are not described by models of continuum mechanics. From our point of view, the main reason for the transformation of the translational directed

motion into a rotational mode is force acting through a distance on the mesoparticle which moves as a solid.

In Section 4, we briefly describe the theoretical approach developed in [16,17] to describe highly non-equilibrium processes based on the rigorous results of non-equilibrium statistical mechanics. The approach allows us to consider the medium response to external influence as a result of the dynamics of the non-equilibrium spatiotemporal correlations on the mesoscale.

Then, in Section 5, we show how the approach explains the turbulence occurrence.

In Section 6, we show the physical nature of the experimentally observed motions on the mesoscale in the form of some quasi-particles formed by the fragmentation of spatial correlations upon impact on the material. Only formations such as wave packets can propagate in a dispersed medium and transfer mass and momentum.

In Section 7, the energy exchange between two different scales is considered. The experimentally detected energy loss of the shock-induced waveform generated at high-rate deformation is explained by the transition of a part of the energy to a lower scale. Due to the transition, the average velocity of deterministic motion at a higher level decreases and the chaotic pulsation modes at a lower level grow. For this, it was necessary to redefine the concept of energy for the transport processes far from local equilibrium.

2. Experimental Research on Shock Loading of Solids

Experimental research on shock loading of metals [2–4] has shown that the propagation of shock-induced waveforms has much in common with the motions of wave packets. In the experiments on shock loading of solids, such wave packets were detected simultaneously at two scales: meso-1 and meso-2. The mesoparticles-1 are wave packets generated during the scattering of the initial compression wave on the crystal structure of the material. The mass velocity dispersion as standard velocity deviation, $\left\langle v^2 - \langle v \rangle^2 \right\rangle = D^2(\zeta)$, is recorded in real time inside the waveform passing through the back side of the metal target. The mass velocity dispersion is recorded on a much smaller scale compared to the waveform itself and therefore can be considered as scatter in the velocities of the medium particles on the mesoscale-1. The waveform itself is recorded at a spot whose diameter coincides to the diameter of the laser beam on the target back side. It is much larger and can be considered as mesoscale-2. The shock-induced waveform recorded experimentally describes a moving particle on the mesoscale-2 which is a superposition of the moving wave packets on the mesoscale-1. The revealed relationships between the mass velocity variance, velocity loss at the wave compression plateau and threshold of structural instability registered in real time testify the momentum and energy exchange between the mesoscale-1 and 2 accompanying the wave transport.

Experiments also show that two different situations are possible. Below a threshold shock velocity, the shocked material is almost entirely restored after shock during the rise time of the plastic front and the mass velocity value at the waveform compression plateau is close to the shock velocity. In Figure 1 the temporal profiles for mean mass velocity and velocity variance in the waveform passing the target are plotted together. This situation corresponds to reversible case when the mass velocity at the pulse plateau equals to the impact velocity. In the case, the mass velocity dispersion is observed only in the middle of the forefront during the rise time. It is rather small; its maximum is reached at the time when the forefront is the steepest.
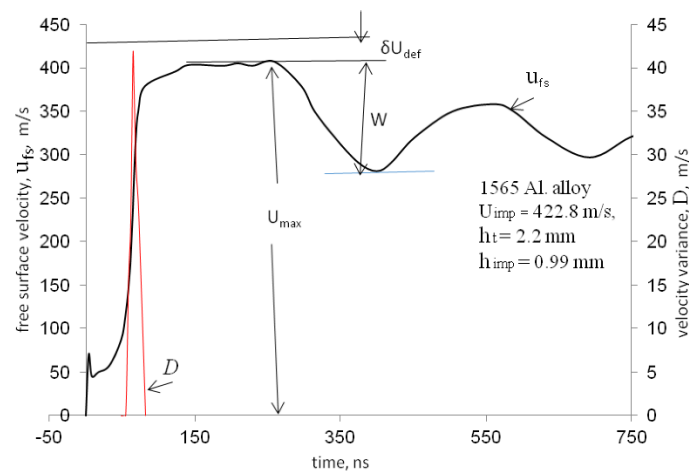
Figure 1. Free surface velocity profile, ufs(t), and velocity variance profile, D(t), for 1565 aluminum alloy target of 2.2 mm thickness loaded at the impact velocity 422.8 m/s.

The experiment shows the synchronous growth of both the strain-rate and variation of the mass velocity in the middle of the wave forefront (see Figure 1). As in turbulent fluid flows [18], there is the proportionality between the variation in mass velocity and the strain-rate $D \sim de/dt$. The relationship establishes a connection between the variation in mass velocity D describing the average amplitude of the mass velocity pulsations on the mesoscale-1 and the strain-rate during the deformation inside the waveform on the mesoscale-2.

However, when the impact velocity exceeds the threshold value, the velocity variance grows drastically (see Figure 2). In the case of shock loading, the mass velocity loss on the waveform plateau is called the mass velocity defect. An independent measurement of the free surface velocity U_f and the projectile velocity V_0 during its collision with the target allows its determination.
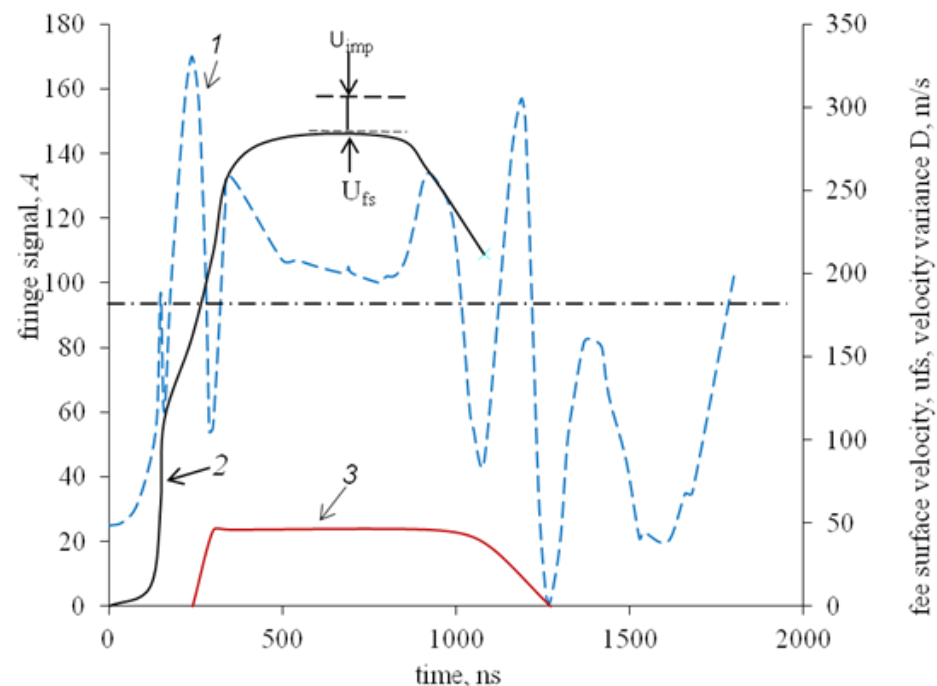

Figure 2. Interference signal (1), time-resolved velocity profile (2) and velocity variance (3) for the shock loading of a 5 mm 38CrNi4Mo steel target at an impact velocity of 320 m/s. Velocity defect equals to difference between velocity of impactor, Uimp, and maximum free surface velocity, Ufs.

In a symmetric collision, the mass velocity in an elastic wave is equal to half the projectile velocity. On the free surface the wave amplitude doubles. If the material state is entirely restored after the shock, the waveform amplitude on the plateau should be equal to the projectile velocity $U_f = V_0$. Due to the interaction of the wave packets, the energy exchange between different scales causes the loss of some kinetic energy in the waveform. In this case, the mass velocity defect is determined as the difference between the projectile velocity and the maximum value of the free surface velocity on the compression pulse plateau $\Delta U = V_0 - U_f$. The value of this defect indicates how much the material state can recover during the rise time after the energy transition to the mesoscale-1. The material state not completely recovered after shock is unstable; the dynamic structure on the mesoscale-1 inside the propagating waveform may partially disappear and partially remain in the trail after passing the waveform. The magnitude of the velocity defect can depend on many factors such as the initial state of the material internal structure, the strain-rate during loading, and the aptitude of the material to structural and phase transformations, etc. Numerous examples of the mass velocity behavior in experiments with different materials in a wide range of loading conditions are presented in the monograph [2].

Unlike the case presented in Figure 1, when the mass velocity dispersion remains almost constant on the pulse plateau (see Figure 2), the waveform amplitude on the mesoscale-2 falls significantly but the velocity dispersion increases greatly. This means that a considerable amount of kinetic energy remained on the mesoscale-1 during the mass velocity pulsations; the material state was not restored after the shock inside the waveform and was unable to maintain the stress induced by the impact. The energy exchange between the scales meso-1 and meso-2 was irreversible.

Experiments [2] show that such a situation can arise in a threshold manner with an increase in the impact speed. In Figure 3, the dependence of the maximum free surface velocity at the plateau of compressive pulse on the impact velocity is provided.
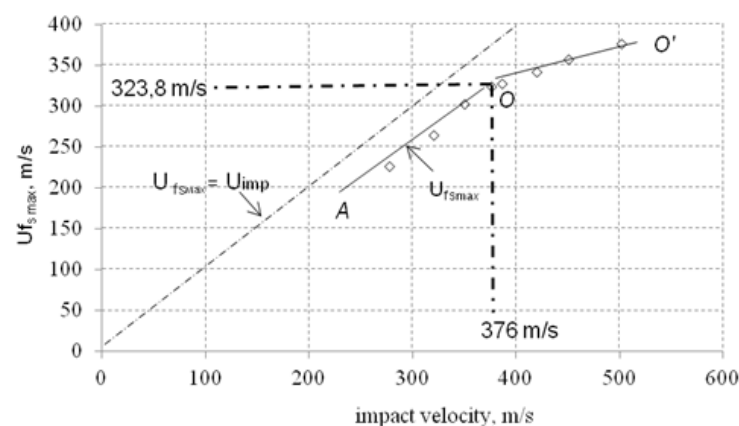

Figure 3. Dependence of the maximum free surface velocity, Ufs max, on the impact velocity for 38CrNi3MoV steel. Dotted line at 45° corresponds to equality of the free surface velocity to impact velocity under symmetrical collision. Transition to structure-unstable state occurs at the impact velocity of 376 m/s.

It is the simultaneous registration of both the mass velocity inside the waveform on the mesoscale-2 and its variations in real time that makes it possible to obtain information about the character of the energy exchange between the mesoscale-1 and the mesoscale-2 at different stages of high-rate deformation. The measured defect of the mass velocity at the plateau of the compression pulse is a quantitative characteristic of the energy exchange. Structural transformations of the material under high-rate deformation change its initial state, either reversibly or irreversibly, depending on strain-rate. The irreversible change induces the loss of momentum and energy of the waveform, as a result of which the material after the passage of the waveform acquires a new internal structure and new mechanical properties.

So, the most important characteristics of the dynamic deformation and fracture of materials are not only the dynamic yield point, the threshold for structural instability, and spall strength, but also the mass velocity defect. Due to the exchange processes, the material during high-rate deformation achieves a structure-unstable state, in which there emerges a synergetic genesis of the three-dimensional pulsations and rotations observed experimentally. This means that the presence of an initial structural inhomogeneity in the material with an increase in the strain rate leads to a transition to the turbulent mode of the motion of mesoparticles in the material.

3. The Physical Nature of the Turbulent Movement

Turbulence is the most common form of motion of a real medium and the practical importance of developing adequate theoretical models and experimental studies of turbulence is difficult to overestimate. However, the problem of turbulence still remains one of the most important unsolved problems of classical physics. Over the past decades, scientists have not been able to find a reliable way to predict the behavior of turbulent motions. Therefore, understanding the nature of turbulence and developing methods for its adequate modeling are the most important tasks of modern physics.

It is generally accepted that the origin of turbulence is the high-speed interaction of the medium with interphase boundaries, close to which large spatial gradients of mass velocity arise [19–23]. In the transition to the turbulent mode of motion, the diffusion mechanisms of momentum transfer are replaced by convective and wave ones, and dissipative effects are superseded by inertial ones. In [24], it is shown that the shear motion of the medium, based on the viscous interaction of layers, cannot be stable at large spatial velocity gradients and must be converted into rotational motion through the formation of vortex structures.

From the point of view of thermodynamics, strong spatial inhomogeneity corresponds to a significant deviation of the system state from local thermodynamic equilibrium. However, as is known, the thermodynamics of macroscopic systems is based on the concept close to thermodynamic equilibrium. All attempts to generalize the known models of continuum mechanics to essentially non-equilibrium processes by adding non-linear terms, higher gradients or additional effects, as practice has shown, deliberately narrow their validity and deprive them of predictive ability.

The greatest deviations of the medium state from thermodynamic equilibrium are caused by the transformation of the directed motion of the medium into rotational mode. In this case, it is necessary to understand how a strong shear generates a vortex.

In Figure 4, a transition of shear band into rotation cell for a shock-loaded VT14 titanium alloy is presented.

The moment of inertia of a rigid body I is a quantity that determines the torque $\mathbf{M}$ needed for a desired angular acceleration $d\omega/dt$ about a rotational axis, similar to mass in the relationship between force and acceleration. Spin angular velocity ω refers to how fast a rigid body rotates with respect to its center of rotation and is independent of the choice of origin, in contrast to orbital angular velocity. The torque on a point particle $\mathbf{M}$, which has the position $\mathbf{r}$ in some reference frame, can be defined as the cross product of the vector $\mathbf{r}$ and the force vector $\mathbf{F}$: $\mathbf{M} = \mathbf{r} \times \mathbf{F}$ **F: M = r × F.** The magnitude of the torque of a rigid body depends on the force applied, the lever arm vector connecting the point about which the torque is being measured to the point of force application, and the angle between the force and lever arm vector. The net torque on a body determines the rate of change in the angular momentum $\mathbf{L}$ of a body: $\mathbf{dL/dt=M}$, $\mathbf{L} = \mathbf{r} \times \mathbf{p}$ ($\mathbf{p}$ is the particle momentum).

In Figure 5, we can see that the shock-induced rotational cells are formed by the joint action of intrinsic (spin) and orbital torque, which causes rotations and the curvature of the trajectory of the medium motion. In both cases, the rotation is the result of a force applied not at a given point, but through a distance that forms the arm of the force. In a rigid body, all its points are linked and move keeping their positions relative to each other. Deformation changes the relative positions of the medium particles, and their movement loses part of their correlations. Gas particles move chaotically, keeping only correlations

between movements at a mean velocity on the macroscale. Between the two limiting cases the correlated movement remains on the intermediate scale between micro and macro, called mesoscale, when mesovolumes move as separate solids. Their interaction generates an inhomogeneous field of velocities that induces forces applied through the mesoscopic distance to the surfaces of the mesoparticles.
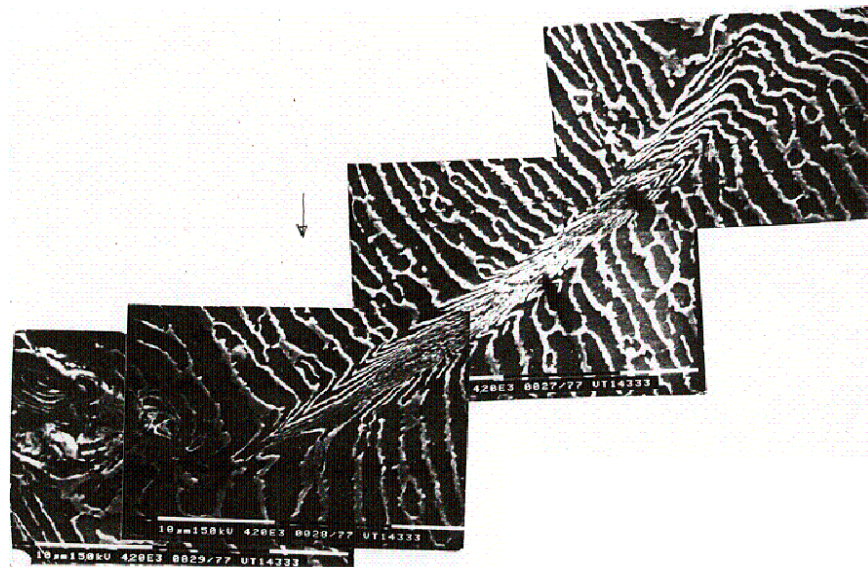

Figure 4. Transition of shear band in shock-deformed VT14 titanium alloy target into rotation.
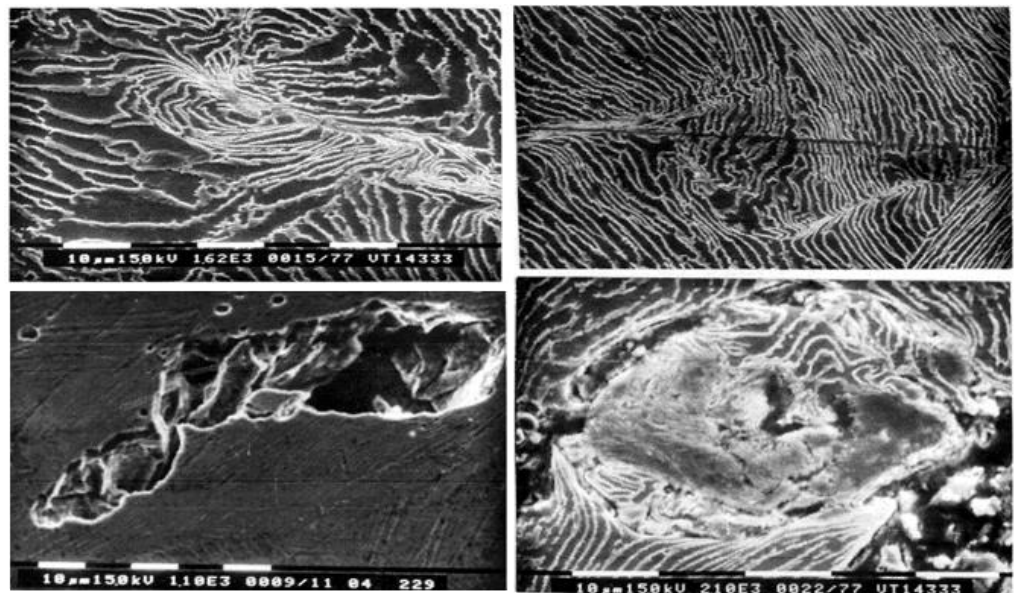
Figure 5. The rotational cells in shock-deformed VT14 titanium alloy targets.

Thus, for the occurrence of rotational motions, the presence of spatially correlated motions is necessary when finite volumes of a medium of any nature move as solid bodies with different shift velocities. In Figure 6, the rotation cells in shock-deformed copper obtained by simulation are presented [25]. In Figure 7, the experimentally observed rotation cells are provided for comparison.
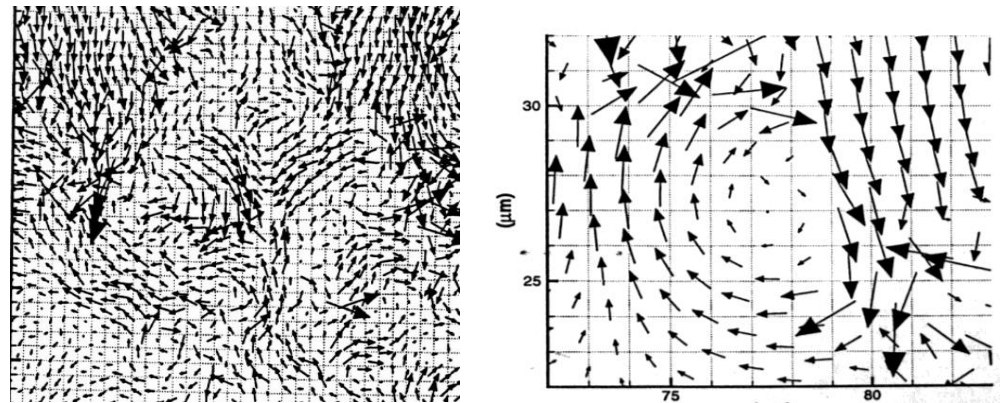
Figure 6. Velocity heterogenization of shock-loaded polycrystalline copper.(after Yano K., Horie Y-Y).

Figure 7. The rotational cells in the spall zone in steel 4340 at the impact velocity 343 m/s.(enlarged 1000+).

The dynamic strength of material strongly depends on the density of rotational cells. In Figure 8, the experimentally obtained dependencies of spall strength and density of rotational cells on the impact velocity are presented. Both dependencies are non-monotonous, and the spall strength maximum coincides with the maximum of rotational cells' density.

Figure 8. Dependencies of spall strength, *W*, and density of rotational cells. On the impact velocity for 2Cr-2Ni-Mo-V steel 4.

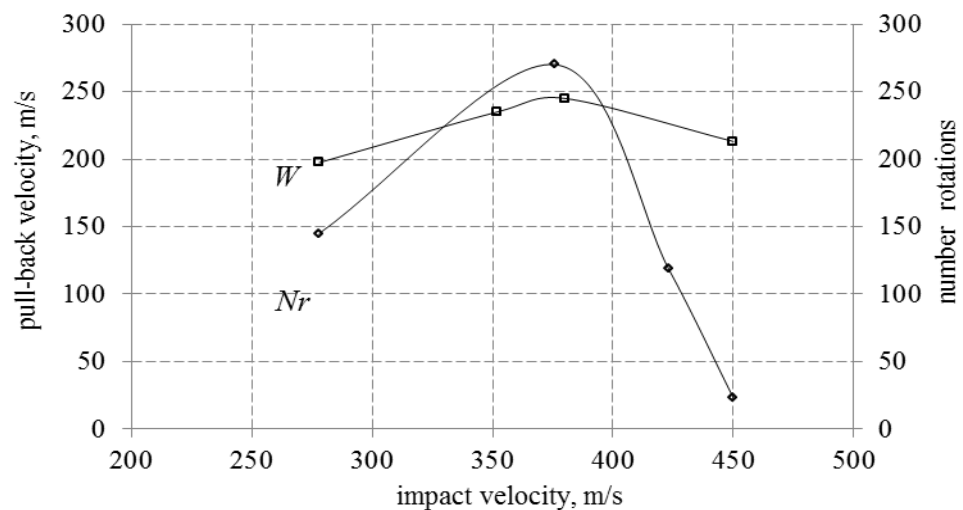If a force is allowed to act through a distance, it is conducting mechanical work. Similarly, the torque acting through a rotational distance is also conducting work. For some time intervals, the work is not converted into heat [13,15] but remains on the mesoscale in the form of kinetic energy due to the inertia of the medium. To maintain the rotational motion of mesoparticles, their moments of inertia play an important role. In this case, a part of the shock-induced kinetic energy on the macroscale is lost. A similar situation is observed for turbulent processes of any nature.

So, the occurrence of turbulence indicates significant deviations of the system states from the local thermodynamic equilibrium. Far from thermodynamic equilibrium, as experiments show, transport processes are often accompanied by the effects of self-organization observed in different media on the intermediate scales between macro and micro that are determined not only by their initial structure and phase state but also by the loading and boundary conditions, and by the integral properties of the system such as its size and geometry.

The interaction between the structure elements causes the formed structures to evolve. The rate of the structure evolution and retarding responses to the external actions could affect the relaxation characteristics of medium and lead to system instability, fluctuations, structural transformations, switching from one regime to another and to origin feedbacks. Manifestations of strong non-equilibrium of processes associated with the formation of turbulent structures are inherent not only in flows of liquid media, as experiments show, but also in solids under high-speed deformation.

Such experimentally observed features of non-equilibrium processes cannot be described within the framework of continuum mechanics and require developing a principally new approach based on rigorous results of non-equilibrium statistical mechanics.

4. Nonlocal Approach to Describe Turbulent Motion

From the viewpoint of non-equilibrium statistical mechanics, in case of arbitrary deviation from local equilibrium state, any scale level of averaged description of a system is incomplete. Therefore, one of the most important results of non-equilibrium statistical mechanics is a proof of the fact that equations describing a behavior of a non-equilibrium statistical system in terms of an incomplete set of variables cannot be differential, i.e., connecting quantities at the same spatial point and at the same moment in time (i.e., local both in the space and time) [26–30].

A fruitful statistic-mechanical method to describe non-equilibrium transport processes of mass, impulse and energy was proposed by D.N. Zubarev [31–33]. The obtained approach within the thermodynamic relationships between conjugate fluxes $\mathbf{J}(\mathbf{r}, t)$ and macroscopic density gradients of impulse and energy $\mathbf{G}(\mathbf{r}, t)$ are integral both in space and time. They include relaxation transport kernels $\mathbf{K}(\mathbf{r}, \mathbf{r}', t, t')$, which generalize the transport coefficients to non-equilibrium conditions

$$\mathbf{J}(\mathbf{r}, t) = \int\limits_{-\infty}^{t} dt' \int\limits_{V} d\mathbf{r}' \mathbf{K}(\mathbf{r}, \mathbf{r}', t, t') \mathbf{G}(\mathbf{r}', t') \tag{1}$$

For the high-rate processes, when mechanical energy has no time to dissipate into heat, the cross processes can be neglected. Unlike the transport coefficients, the relaxation transport kernels are nonlinear functionals of macroscopic gradients during the whole history of the transport process. On intermediate scales between micro and macro, it is impossible to divide the processes into scales in advance and the integral kernels can be considered as spatiotemporal correlation functions of macroscopic gradients. Attempts to construct empiric models of the integral kernels led to such coarse description that obviously did not allow satisfying boundary conditions. These obstacles discourage the use of nonlocal models in practical tasks.

On the basis of the nonlocal and retarded transport equations obtained within the non-equilibrium statistical method [31,33], a new self-consistent nonlocal approach to consider

transport processes in open systems was proposed [16,17]. Within the approach, the mathematical model of the spatiotemporal correlation function with parameters evolving in time and characterizing the size of dynamic structure elements was constructed. According to the model, the process of smoothing the gradients of macroscopic fields proceeds with time through the correlation functions in any macroscopic system far from local thermodynamic equilibrium. In the process of smoothing the gradients, dynamic structures in the form of clusters with almost identical values of macroscopic densities will form in the system. The finite-size clusters move as nearly solid particles that can interact and rotate. The sizes of these cluster structures can vary over a very wide range between micro and macro scales. This intermediate level is considered to be mesoscopic. The interaction of such mesoparticles leads to the system evolution described by cybernetic methods developed within the control theory of adaptive systems via close-loops [34,35]. Over time, these clusters will grow and merge with each other, reducing their number in the system, until they form one cluster with the same equilibrium values of some densities, if this is allowed by the imposed constraints.

Like in quantum mechanics, the boundary conditions imposed on the system lead to the discretization of the size spectrum of the internal structure (structuring of system) [17,36]. By means of the structure parameters, the boundary problem formulation for the nonlocal equations becomes self-consistent: the transport process depends on the structure of a system, whereas the structure, in turn, is determined by the transport process itself. The close-loops between structure evolution and the regime of loading are incorporated in the model.

We can conclude that such a multi-disciplinary synthetic approach at the crossroads of mechanics, physics and cybernetics can describe high-rate turbulent transport processes in an open system of various natures. In the next section, we show how the correlation dynamics on the mesoscale generates turbulence.

5. Turbulence Generation by Non-Local Correlations

The mesoscopic structure of the medium, generated by external influences that significantly deviate the state of the system from local thermodynamic equilibrium, is determined by the dynamics of space-time correlations in the integral kernel $\mathbf{K}(\mathbf{r}, \mathbf{r}', t, t')$. In the study of turbulence, the momentum transfer mechanism is of greatest interest. For simplicity, we first consider the effects of only spatial correlations. For the case of momentum transport, the relationship (1) between the momentum flux $\mathbf{J}$ and the mass velocity gradient $\partial \mathbf{u}/\partial \mathbf{r}$ takes the form

$$\mathbf{J}(\mathbf{r}, t) = \int_V d\mathbf{r}' \mathbf{R}(\mathbf{r}, \mathbf{r}') \cdot \frac{\partial \mathbf{u}}{\partial \mathbf{r}'}(\mathbf{r}') \tag{2}$$

Here, $\mathbf{R}$ is a rank 4 tensor. Its convolution with the rank 2 tensor $\partial \mathbf{u}/\partial \mathbf{r}$ results in the rank 2 tensor $\mathbf{J}$. In order to understand how dynamic mesoparticles are formed, it suffice to consider the properties of the spherical part of the tensor $\mathbf{R}$, $\Psi(\mathbf{r}, \mathbf{r}') = Sp\mathbf{R}(\mathbf{r}, \mathbf{r}')$, which is a scalar function of non-equilibrium spatial correlations. The expansion of the integrand $\partial \mathbf{u}/\partial \mathbf{r}'$ in a Taylor series in a vicinity of the point $\mathbf{r}' = \mathbf{r}$, followed by its substitution under the integral (2), leads to the transition from an integral operator to a differential operator of infinite order

$$\int_V d\mathbf{r}' \Psi(\mathbf{r}, \mathbf{r}') \cdot \frac{\partial \mathbf{u}}{\partial \mathbf{r}'}(\mathbf{r}') = k_0(\mathbf{r}) \cdot \frac{\partial \mathbf{u}}{\partial \mathbf{r}}(\mathbf{r}) + \mathbf{k}_1(\mathbf{r}) \cdot \frac{\partial}{\partial \mathbf{r}} \frac{\partial \mathbf{u}}{\partial \mathbf{r}}(\mathbf{r}) + \frac{1}{2} \mathbf{k}_2(\mathbf{r}) \cdot \frac{\partial^2}{\partial \mathbf{r} \partial \mathbf{r}} \frac{\partial \mathbf{u}}{\partial \mathbf{r}}(\mathbf{r}) + \dots \tag{3}$$

The coefficients in the expansion (3) can be called n-order moments of the spatial correlation function Ψ [12]

$$\mathbf{k}_n(\mathbf{r}) = \int_V \Psi(\mathbf{r}, \mathbf{r}') \underbrace{(\mathbf{r}' - \mathbf{r}) \dots (\mathbf{r}' - \mathbf{r})}_{n} d\mathbf{r}' \tag{4}$$

The moments are *n*-rank tensors. The first three moments have a physical meaning. The 0-order moment $k_0(\mathbf{r}) = \int_V \Psi(\mathbf{r}, \mathbf{r}')d\mathbf{r}'$ generalizes the medium viscosity μ to the case when empiric coefficients under non-equilibrium conditions become dependent on the system sizes and geometry. The 1-order moment

$$\mathbf{k}_1(\mathbf{r}) = \int_V \Psi(\mathbf{r}, \mathbf{r}')(\mathbf{r}' - \mathbf{r})d\mathbf{r}' = \boldsymbol{\beta}(\mathbf{r}) \tag{5}$$

defines a vector. Near the local equilibrium $\Psi(\mathbf{r}, \mathbf{r}') = \delta(|\mathbf{r}' - \mathbf{r}|)$ the vector disappears $\boldsymbol{\beta}(\mathbf{r}) = 0$. This means that out of local equilibrium, new direction and new typical length generated by non-equilibrium correlations make the system anisotropic and give rise to the medium polarization along the direction of the vector $\boldsymbol{\beta}(\mathbf{r})$. The 2-order moment $\mathbf{k}_2(\mathbf{r}) = \int_V \Psi(\mathbf{r}, \mathbf{r}')(\mathbf{r}' - \mathbf{r})(\mathbf{r}' - \mathbf{r})d\mathbf{r}'$ is a rank 2 tensor. Its spherical part

$$\int_V \Psi(\mathbf{r}, \mathbf{r}')(\mathbf{r}' - \mathbf{r})^2 d\mathbf{r}' = \int_V \Psi(\mathbf{r}, \mathbf{r}')(\mathbf{r}'^2 - \mathbf{r}^2)d\mathbf{r}' - 2\mathbf{r}\cdot\boldsymbol{\beta}(\mathbf{r}) = \varepsilon^2(\mathbf{r}) - 2\mathbf{r}\cdot\boldsymbol{\beta}(\mathbf{r}) \tag{6}$$

defines the dispersion ε^2 of the space correlation distribution, which becomes eccentric due to $\boldsymbol{\beta}(\mathbf{r})$. Parameters $\boldsymbol{\beta}$ and ε have the dimensions of length and depend on the system size and its geometry. The medium element of the typical finite size ε moving as an eccentric cluster in inhomogeneous velocity and stress fields should rotate as a whole. Such mesoscale rotations can be considered as the finite size dynamic structure of the bounded system in the volume *V*. On the other hand, if a rotating body moves in a stationary medium, then in addition to the resistance force, another force will act-the Magnus force, which can cause a sharp change in the trajectory of movement. In contrast to the intrinsic rotation (spin) of the mesoparticles, the correlation function generates the lever arm vector $\boldsymbol{\beta}$ connecting the point r with the inertia center of the mesoparticle, to the surface of which the force acting from other mesoparticles is applied. As a result, both the spin of the mesoparticle $\mathbf{S} = \varepsilon \times \mathbf{F}$ (ε is the vector connecting the inertia center of the mesoparticle with the point of the force application, $|\varepsilon| = \varepsilon$ is the typical radius of the mesoparticle) and its orbital rotation $\mathbf{M} = \boldsymbol{\beta} \times \mathbf{F}$ around the point $\mathbf{r}$ with the typical lever arm vector $\boldsymbol{\beta}$ are induced. Here, the division of the angular momentum into spin and orbital is purely arbitrary, since such a division cannot be correctly made for mesoparticles that are not completely solid.

Since the parameters $\boldsymbol{\beta}$ and ε are integral values, their dependence on the point $\mathbf{r}$ should be weak, which makes it possible to use their average values over a certain area tied to the predominant velocity gradients. For the case of the quasi-stationary process, the parameters should be time-dependent. The asymmetric distribution of spatial correlations due to the shift parameter $\boldsymbol{\beta}$ leads to the polarization of the medium with large gradients.

The contribution of this rotational motion to the momentum flux $\mathbf{J}$ is determined by the second and third terms in the expansion (3). However, three terms of the series (3) are not equivalent to the integral operator on the left. In order to preserve the integral description within the framework of the developed nonlocal approach [17], a model correlation function was proposed as the integral kernel in the thermodynamic relationships (2):

$$\mathbf{J}(\mathbf{r}, t) = \frac{k_0}{\varepsilon} \int_V d\mathbf{r}' \exp\left\{-\frac{\pi(\mathbf{r} - \mathbf{r}' + \boldsymbol{\beta})^2}{\varepsilon^2}\right\}\frac{\partial \mathbf{u}}{\partial \mathbf{r}'}(\mathbf{r}') \tag{7}$$

If the size of mesoparticles and the arm vector length are small, the mesoparticle spin can be neglected, while the torques at small angles of rotation can be considered as velocity pulsations. A high-frequency change in the vector $\boldsymbol{\beta}(t)$ causes the oscillatory motions of the medium. Furthermore, it is necessary to keep in mind that the correlation function is tensor, each component of which generates its own vector $\boldsymbol{\beta}$.

Obviously, the occurrence of rotational motions on the mesoscale will reduce the average translational momentum transfer on the macroscale. Associated with this is a decrease in the entropy production in a turbulent flow compared to a laminar one at the same high velocity and the replacement of dissipation by inertial effects during the transition to a turbulent mode of the medium motion [37–39]. Such non-classical effects in a neutral medium can arise only due to nonlocality and lead to asymmetry of the stress tensor [40], near-boundary anisotropy, and ultimately to turbulence.

So, out of local equilibrium, i.e., at high-rates and high gradients, the spatial nonlocal correlations generate the self-organization of turbulent structures.

6. The Nature of Shock-Induced Mesoparticles

Within the proposed approach, mathematical modeling shock-wave processes was developed in papers [17,41]. An explicit solution to the problem on the planar shock –induced wave propagation in solid material was obtained [41]. For the planar shock loading of moderate intensity when the induced wave propagates along x-axis in a linear approximation with respect to the parameter $u/C << 1$, in the reference connected to the elastic precursor of an elastic-plastic wave running at the constant longitudinal sound velocity C, $\zeta = (t - x/C)/t_R$, $\xi = x/L$ (t_R is the loading duration, L is typical distance traveled by the wave), the normalized stress component $P_{xx}/\rho_0 C V_0 = \Pi(\zeta; \tau(\xi), \theta(\xi)) = u(\zeta; \tau(\xi), \theta(\xi))$. ($V_0$ is the shock velocity, u is the induced mass velocity) is determined by the integral equation

$$u(\zeta; \tau(\xi), \theta(\xi)) = \int_{o}^{\omega(\zeta)} d\zeta' \exp\left\{ -\frac{\pi(\zeta - \zeta' - \theta(\xi))^2}{\tau^2(\xi)} \right\} \frac{\partial u(\zeta', \xi = 0)}{\partial \zeta'},$$

$$\omega(\zeta) = \begin{cases} \zeta, & \zeta < 1, \\ 1, & \zeta \geq 1. \end{cases} \tag{8}$$

Equation (8) contains the parameters of relaxation, retardation and nonlocality $\tau = t_r/t_R$, $\theta = t_m/t_R$, $\varepsilon = Ct_r/L$ respectively. The equation was derived under the condition $\tau\partial/\partial\zeta >> \varepsilon\partial/\partial\xi$ resulting from the experimentally tested evaluation $\varepsilon/\tau = Ct_R/L << 1$, which separates fast and slow processes in scales as required for the self-organization of new structures in the medium [42,43]. For extremely short impact, when $\partial u(\zeta', \xi = 0)/\partial\zeta' = \delta(\zeta - \zeta')$, the waveform is Gaussian

$$\Pi(\zeta; \tau(\xi), \theta(\xi)) = \exp\left\{ -\frac{\pi(\zeta - \theta(\xi))^2}{\tau^2(\xi)} \right\} \tag{9}$$

The solution (8) describes both the formation of the so-called elastic precursor and plastic front and the waveform evolution during its propagation along the target material, which has not been studied previously experimentally or theoretically. The obtained solution allows an explanation of experimentally measurable quantities such as the dispersion of the mass velocity and the velocity loss on the plateau of the compression pulse from the viewpoint of the correlation dynamics and provides new opportunities to connect their behavior with the process of turbulent structure formation.

When the shock breaks the long-range order of initial space-time correlations in the solid, the short-range order is retained. Its finite-size parts retained by correlations move as whole particles at different velocities. These mesovolumes exist only inside the waveform as dynamic field formations propagating along the medium and transporting mass, momentum and energy. After the waveform passage, the velocities of the mesoparticles equalize, they merge into one and the material becomes a continuous medium.

The time interval during which the shock impulse is transmitted to the target material is very small (about 10^{-8} s) so that the discrete atomic structure of the solid material scatters the compression wave in velocities forming wave packets on the mesoscale-1. These wave packets become mass and momentum carriers.

The superposition of harmonic waves with a small scatter in wave numbers $\delta k/k_0 << 1$ forms the wave packet with the amplitude $B(x - v_0 t)$

$$\Omega(x,t) = B(x - v_0 t)e^{i(k_0 x - \omega_0 t)} \tag{10}$$

The main maximum of the packet travels at a group speed $v_0 = \dfrac{d\omega}{dk}(k_0)$ which is always less than the phase one. The spatial extent of the packet is determined by the spread in wave numbers $\delta x \sim 1/\delta k$.

Gaussian or normal distribution of the particle coordinate determines the minimum value of the coordinate and momentum uncertainty $\Delta x \Delta p$. These special properties of the Gaussian function play an important role in quantum theory [44].

The function B in the expression (10) for Gaussian wave packet with maximum in the point x_0 moving at the group velocity v_0 has a form

$$B(x) = \frac{1}{\sqrt{2\pi\sigma^2(t)}} \exp\left(-\frac{(x - x_0 - v_0 t)^2}{2\sigma^2(t)}\right) \tag{11}$$

In the linear approximation in k, the shape, size and variance $\sigma(t) = \sigma_0$ remain constant. Accounting for quadratic term k^2 leads to spreading of the wave packet over time. Although its width grows, the Gaussian shape of the wave packet is maintained over time. In this case, the greater the particle mass m, the slower the spreading of the wave packet.

In the frame of reference moving with phase velocity C each point of the spreading packet moves at its own speed. In the time representation in terms of the wave variable $\zeta = t - x/C$ a time shift for each point ζ' and a retardation θ due to the interaction with potential inhomogeneities of the material during the wave propagation are introduced. As a result, the wave packet takes on the form

$$B(\zeta) = \frac{1}{\sqrt{2\pi\sigma^2(t)/v_0^2}} \exp\left(-\frac{(\zeta - \zeta' - \theta)^2}{2\sigma^2(t)/v_0^2}\right) \tag{12}$$

which, up to a normalization factor, coincides with the form of the model correlation function in the relationship (8).

Now, we can assume that the shock-induced mesoparticles as part of the material retaining spatial correlations on the mesoscale upon impact are the wave packets that are capable of transporting mass, momentum and energy. The chaotic component of their motion recorded experimentally as the mass velocity variance on the mesoscale-1 reduces the observed stress magnitude. However, over time, the material tends to return to its original state. When the wave packet motions become more organized, the observed stress magnitude grows. It is possible due to the inertia of the medium, since the post-shock effects allow the stress to recover for some time. This effect is known as the plastic front rise. It must be noticed that the recovery of the initial solid state over the risetime has nothing to do with plasticity. This wrong term appeared as a result of a misunderstanding of the physics of the process [45].

The experimentally observed shock-induced waveform is a superposition of the interacting wave packets on the mesoscale-1 that form a much larger packet on the mesoscale-2.

$$v(\zeta) = \sum_i^n \Pi_i(\zeta; \tau_i, \theta_i) \approx \int_0^\omega d\zeta' \exp\left\{-\frac{\pi(\zeta - \zeta' - \theta(\xi))^2}{\tau^2(\xi)}\right\} \tag{13}$$

The wave packets' interaction can considerably enhance the scatter in their velocities, which can lead to strong shears and, consequently, to the occurrence of rotational modes. In this case, the motion of the mesoparticles can become turbulent. Unlike turbulence in liquids, where the greatest contribution to the entropy production is due to dissipation, the inertial properties of the solid material decrease the entropy production in the waveform

and even make it negative due to the self-organization of turbulent structures during its high-rate deformation [17]. After the passage of the front, the formed turbulent structures partially remain frozen into the material and are observed in the targets as the shock-induced structural defects (Figures 4, 5 and 7).

The reversible part of the mesoparticles motion cannot be seen. However, it is possible to see the mesoparticles in conditions when they are instantly removed from one another, so there is no time for their velocities to equalize. The conditions are realized within the spall zone of shock-deformed material, where for a very short time, comprehensive tension stress is induced. During spallation, the spall surfaces of the target are quickly removed from each other, conserving the structure of the material inside the spall zone. In this case, the boundaries between the mesoparticles, which separate the volumes of the medium with different velocities, are also conserved.

Some typical relict mesostructures are presented in Figure 9. A powder with a vortex internal structure was found in the spall zone of copper targets after shock loading.
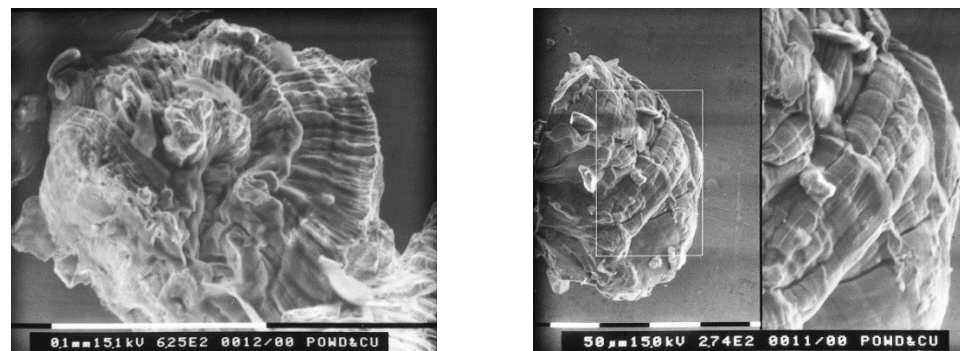

Figure 9. Relict crystallized mesoparticles with shear bands within spall zone. Of shock-deformed copper (chapter 4 [2]).

The waveforms interaction and their scatter by the defects of the material structure on the mesoscale-2 increase their delays and wavelength. The experimentally observed waveforms on the mesoscale-2 spread out when moving through an inhomogeneous material [41] like the wave packets in quantum mechanics [44].

7. Energy Exchange between Meso-1 and Meso-2 Scales

Of greatest interest are the experimental results on the correlation of data at different scales [2]. The observed patterns between the evolution of the mass velocity waveforms and the microstructural changes in the medium during the passage of the wave indicate the consistency of the exchange processes between different scale levels. In the general case, the kinetic energy of the projectile transforms into rotational-shear wave structures on the mesoscale through a hierarchy of scale levels and partially dissipates into the thermal component of the internal energy of the material. Due to multi-scale and multi-stage energy exchange between different-scale impulse carriers, chaotic pulsation modes at a lower level reduce the average velocity of deterministic motion at a higher level [2].

Consider the energy exchange between two scale levels, mesoscale-1 and mesoscale-2. To do this, we need to use the results obtained for the shock-induced planar elastic-plastic wave propagating in condensed matter [41]. In the considered case the energy transport equation for shock-induced processes is written in the running reference frame as follows

$$\frac{\partial E}{\partial \zeta} = \Pi(\zeta, \xi)\frac{\partial u}{\partial \zeta}(\zeta, \xi) \tag{14}$$

The traditional transport Equation (14) determines volumetric internal energy density $E(\zeta, \xi)$. However, when the stress $\Pi(\zeta, \xi) = u(\zeta, \xi)$ (elastic stress is proportional to strain u/C) and the strain-rate $\frac{V_0}{C}\frac{\partial u}{\partial \zeta}(\zeta)$ are given at the same instant ζ and point ξ, thus defined

energy coincides with elastic energy $E = u^2/2$. In the case, the process of all its transformations within the shock-induced waveform is entirely reversible, which contradicts the experimental studies on shock loading [2–4]. This means that, like other thermodynamic quantities determined in close-to-equilibrium conditions, the concept of energy is to be redefined for the highly non-equilibrium processes.

It is fundamentally important that the work of the deformation forces is performed only during the loading time interval, while the relaxation in the medium due to inertia can be regarded as a post-effect that propagates in the medium in the form of a wave. The shock-induced waveform propagation is nonlocal process in which the stress and strain-rate are related to each other at different spatial points and time instants. The strain-rate during the loading at the impact surface generates most parts of the stress much later when the waveform has already traveled some distance from the impact surface. Far from local equilibrium, the energy is distributed between different degrees of freedom unevenly and the kinetic energy of vibrations is not equal to the potential one.

Instead of Equation (14), the internal energy at any instant during and after the shock is defined by the deformation work in non-equilibrium conditions as follows

$$E = \int_0^\zeta \Pi(\zeta; \tau(\xi), \theta(\xi)) \frac{\partial u_0}{\partial \zeta} d\zeta \tag{15}$$

where the normalized acceleration during the shock loading is given $\partial u_0/\partial \zeta = V_0/t_R = 1$, $0 \leq \zeta \leq 1$ and after the shock $\partial u_0/\partial \zeta = 0$, $\zeta > 1$. In the case, the internal energy ceases to be a full differential and a thermodynamic potential

$$E = \int_0^\zeta \Pi(\zeta; \tau(\xi), \theta(\xi)) d\zeta, \ \ 0 \leq \zeta \leq 1$$

$$\text{and} \tag{16}$$

$$E = \int_0^1 \Pi(\zeta; \tau(\xi), \theta(\xi)) d\zeta, \ \ \zeta \geq 1$$

The full differential is the total mechanical energy that can be thermodynamic potential far from local equilibrium

$$\frac{\partial E}{\partial \zeta} = \frac{\partial u_0 \Pi}{\partial \zeta}, \ E = \Pi u_0 = u(\zeta, \xi) u_0(\zeta, \xi = 0) \tag{17}$$

The energy in the form $u(\zeta, \xi) u_0(\zeta, \xi = 0)$ is two-point and two-instant correlation function. The total mechanical energy is the sum of potential and kinetic energies

$$E = \int_0^\zeta \Pi(\zeta; \tau(\xi), \theta(\xi)) \frac{\partial u_0}{\partial \zeta} d\zeta + \int_0^\zeta u_0(\zeta) \frac{\partial \Pi}{\partial \zeta} d\zeta \tag{18}$$

However, individually, these energies, not being full differentials, lose their generally accepted meaning. Far from equilibrium, these energies cannot be equal to each other. Near local equilibrium in fluids and lower the elastic limit in solids when strain-rate induces stress simultaneously at the same point, we return from Equation (15) to elastic energy

$$E_p = E_k = \int_0^\zeta u(\zeta) \frac{\partial v}{\partial \zeta} d\zeta \rightarrow \frac{u^2}{2}, \ \ 0 \leq \zeta \leq 1 \tag{19}$$

Let us calculate the total mechanical energy received by the medium during shock loading and its further evolution using the definition

$$E(\zeta, \xi) = u_0(\zeta, \xi = 0) \Pi(\zeta; \tau(\xi), \theta(\xi)) \tag{20}$$

As a result of the impact, the material acquires the energy $E(\zeta = 1, \xi = 0) = u_0(\zeta = 1, \xi = 0)\Pi(1; \tau(0), \theta(0)) = u_0^2(\zeta = 1, \xi = 0) = 1$. When the wave travels from the shocked surface, the energy inside the waveform first drops fast during the elastic precursor relaxation and then grows during the time interval θ on the plastic front until it reaches the constant value on the pulse plateau $E(\zeta = 1 + \theta; \xi) = u_0(\zeta = 1 + \theta; \xi = 0)\Pi(\zeta = 1 + \theta; \tau(\xi), \theta(\xi)) = \Pi(\zeta = 1 + \theta; \tau(\xi), \theta(\xi))$ where $\zeta = 1 + \theta$ and $u_0(\zeta = 1 + \theta; \xi = 0) = 1$. During the relaxation of the elastic precursor, the energy from the mesoscale-2 travels down to the mesoscale-1 forming interacting wave packets. During the risetime θ of the so-called plastic front, the process travel back from mesoscale-1 to mesoscale-2. If the material state is completely restored after the shock, the stress is equal to its initial value $\Pi(\zeta = 1 + \theta; \tau(\xi), \theta(\xi)) = 1$. In this case, all the energy transformations during the transitions from mesoscale-2 to mesoscale-1 and back were reversible inside the waveform. However, total momentum of the waveform and the total momentum flux can lose some parts due to the relaxation and delay effects of the material state recovery.

In experiments [2], with an increase in the impact velocity, a different situation is observed when the mass velocity defect $\Delta U = 1 - \Pi(\zeta = 1 + \theta; \tau(\xi), \theta(\xi)) \geq 0$ occurs at the waveform plateau. The appearance of the velocity defect at the pulse plateau indicates that the restoration of the initial material state is not completed. This process inside the waveform becomes irreversible, since a part of the full mechanical energy remained on the mesoscale-1 in the form of chaotic mass velocity pulsations

$$E(\zeta = 1, \xi = 0) - E(\zeta = 1 + \theta, \xi) = 3nD^2/2 \qquad (21)$$

Here, $3D^2/2$ is the kinetic energy of the chaotic part of the wave packet motion and n is a number of the wave packets on the mesoscale-1 inside the waveform at the mesoscale-2. For the chaotic movement, the kinetic energy is defined correctly, since it means that on the mesoscale-1 local thermodynamic equilibrium is reached. However, the rotational modes of movements on the mesoscale-1 cannot be expressed in terms of variance D as in (21).

With an increase in the impact velocity and a decrease in the duration of the waveform, the multi-scale relaxation processes of restoring the initial state of the material do not have enough time to reach local equilibrium inside the waveform. When the impact velocity reaches a certain threshold value, the velocity defect on the pulse plateau begins to grow rapidly. This indicates a strong deviation of the system state from local equilibrium inside the waveform. As mentioned in paragraph 6, a strong velocity inhomogeneity at mesoscale-1 inevitably leads to the appearance of rotational modes of motion, which require more energy to remain on the mesoscale-1. Apparently, it can be considered that the transition to turbulent motion of the wave packets begins in the material. As the experiments show, unloading material in such a non-equilibrium state leads to irreversible structure formation in the material after the waveform passing. As a result, the spall strength falls with an increase in the mass velocity defect as the material state becomes less solid [46].

The obtained results confirm that the energy exchange between different scales depends on the stage of development of the turbulent process at a deeper scale level and essentially influences the mechanical properties of the medium.

8. Conclusions

The non-local theory of non-equilibrium transport processes [17], based on the rigorous results of non-equilibrium statistical physics [31,32] on the one hand, and long-term studies of shock-wave processes in condensed media [2–4] on the other, made it possible to take a fresh look at the problem of turbulence. The turbulent nature of motion is characteristic of high-rate processes, not only for liquid and gaseous media, but it also manifests itself even in solids at high strain rates. Although we cannot see turbulent motions directly in a solid, in experiments, it is possible to register in real time such characteristics of motion at different scales that make it available to trace the transition to turbulence.

Within the framework of the theoretical approach, the emergence of mesoparticles as a result of the splitting of spatiotemporal correlations during high-rate deformation of

the medium is substantiated. The first moments of the non-equilibrium spatial correlation function determine the effective radius of the mesoparticle and the shift vector of its center of inertia, which are responsible for its intrinsic and orbital moments of rotation and, accordingly, for the appearance of vortices and twisting of the trajectory of its motion. These properties of mesoparticles depend on many parameters: the strain rate, the pulse duration, the initial structure of the medium, as well as on the integral properties of the boundary conditions, dimensions, and shape of the sample. For a finite system, the number of particles is finite. The actual occurrence of turbulence is explained by the appearance of a lever arm of force acting on a mesoparticle of finite size moving like a solid body from the side of other mesoparticles.

Turbulent structures are an example of discretization of the phase space of a system far from local equilibrium [36]. To describe the evolution of turbulent structures, methods of the control theory of adaptive systems are used (speed gradient principle [34,35]). The predictive ability of such a description is due to the thermodynamic goal function, which corresponds to the desire of the system to respond to external influences with the least losses (minimizing the integral production of entropy in the system) [17].

It is shown that the mesoparticle moves as a wave packet formed in a medium with dispersion, transferring mass, momentum and energy. The interaction of mesoparticles can lead to the formation of larger particles, which further enhance the velocity inhomogeneity in a deformable medium. Such packets are experimentally registered as motions on the mesoscale-1 in the form of the mass velocity variance and as waveforms on the mesoscale-2 in the shock deformed solids. In this case, momentum and energy are transferred to another scale level. To describe the process of energy exchange between them, the total energy density is redefined, because far from local equilibrium, it cannot be correctly divided into kinetic and internal parts. The loss of the wave amplitude recorded at meso-2 in cases where the state of the medium does not have time to recover after the impact is consistent with the increase in the velocity variation recorded at meso-1, which indicates a transition to turbulent motion at meso-1. Due to the rotational motion at meso-1, most of the energy remains at meso-1, while in the experiment, there is a sharp drop in the wave amplitude.

Therefore, we tried to demonstrate in our paper that in order to adequately describe high-speed processes in any medium, the construction of mathematical models should be based on a rigorous theoretical framework that allows us to describe the self-organization and interaction of turbulent structures at different scales.

Author Contributions: Conceptualization, T.A.K.; methodology, T.A.K.; investigation, Y.I.M.; writing—original draft preparation, T.A.K. and Y.I.M.; visualization, Y.I.M. All authors have read and agreed to the published version of the manuscript.

Conflicts of Interest: The authors declare no conflict of interest.

References

1. Kuzemsky, A.L. Temporal evolution, directionality if time and irreversibility. *Riviista Del Nuovo Cim.* **2018**, *41*, 10.
2. Meshcheryakov, Y. *Multiscale Mechanics of Shockwave Processes*; Springer Nature Pte Ltd.: Singapore, 1921; p. 192. [CrossRef]
3. Meshcheryakov, Y.I.; Divakov, A.K.; Zhigacheva, N.I. Shock-induced structural transition and dynamic strength of solids. *Int. J. Solids Struct.* **2004**, *41*, 2349–2362. [CrossRef]
4. Meshcheryakov, Y.I.; Divakov, A.K.; Zhigacheva, N.I.; Makarevich, I.P.; Barakhtin, B.K. Dynamic structures in shock-loaded copper. *Phys. Rev. B* **2008**, *78*, 64301–64316. [CrossRef]
5. Asay, J.R.; Barker, L.M. Interferometric measurements of shock-induced internal particle velocity and spatial variation of particle velocity. *J. Appl. Phys.* **1974**, *45*, 2540–2546. [CrossRef]
6. Chabbildas, L.; Trott, W.M.; Reinhart, W.D.; Cogar, J.R.; Mann, G.A. Insipient spall studies in Tantalum—microstructural effects. In Proceedings of the Shock Compression of Condenced Matter-2001, Pre-Conference: Workshop on Shock Dynamics and Non-Equilibrium Mesoscopic Fluctuations in Solids, Renaissance Waverly Hotel, Atlanta, GA, USA, 23 June 2001.
7. Gupta, Y.M. Shock-wave experiments at different length scales: Recent achievements and future challenges. In *Shock Compression of Condensed Matter-1999*; Furnish, M.D., Chhabildas, L.C., Nixon, R.S., Eds.; American Institute of Physics: Melvill, NY, USA, 2000; pp. 3–10.

8. Vogler, T.J.; Reinhart, W.D.; Chhabildas, L.C. Dynamic behavior of boron carbide. *J. Appl. Phys.* **2004**, *95*, 4173–4183. [CrossRef]
9. Koskelo, A.C.; Greenfield, S.R.; Raisley, D.L.; McClellan, K.J.; Byler, D.D.; Dickerson, R.M.; Luo, S.N.; Swift, D.C.; Tonk, D.L.; Peralta, P.D. Dynamics of the onset of damage in metals under shock loading. In Proceedings of the Shock Compression of Condensed Matter 2007, AIP-955 557-560, Waikoloa, HI, USA, 24–29 June 2007.
10. Morozov, V.A. Features of loading, deformation and fracture of materials in the submicrosecond and nanosecond ranges of durations. In Proceedings of the 14th Internat, School on Continuum Mechanics Models, Dolgoprudny, Russia, 1997; pp. 187–191. (In Russian)
11. Asay, J.R.; Chhabildas, L.C. Paradigms and Challenges in Shock Wave Research. In *High-Pressure Compression of Solids VI: Old Paradigms and New Challenges*; Horie, Y., Davison, L., Thadhani, N.N., Eds.; Springer: Berlin/Heidelberg, Germany, 2003; pp. 57–108.
12. Lee, J. The Universal Role of Turbulence in the propagation of Strong Shocks and Detonation Waves. In *High-Pressure Compression of solids VI: Old Paradigms and New Challenges*; Horie, Y., Davison, L., Thadhani, N.N., Eds.; Springer: Berlin/Heidelberg, Germany, 2003; pp. 121–144.
13. Ravichandran, G.; Rosakis, A.J.; Hodovany, J.; Rosakis, P. *On the Convention of Plastic Work into Heat During High-Strain-Rate Deformation, Proceedings of the Table of Contents Shock Compression of Condensed Matter—2001: 12th APS Topical Conference, Atlanta, GA, USA, 24–29 June 2001*; Furnish, M.D., Thadhani, N.N., Horie, Y.-Y., Eds.; American Institute of Physics: Melville, NY, USA, 2002; pp. 557–562.
14. Panin, V.E.; Egorushkin, V.E.; Panon, A.V. Physical mesomechanics of a deformed solid as a multilevel system. 1. Physical fundamentals of the multilevel approach. *Phys. Mesomech.* **2006**, *9*, 9–22.
15. Bever, M.B.; Holt, D.L.; Titchener, A.L. The stored energy of cold work. *Prog. Mat. Sci.* **1973**, *17*, 5–77. [CrossRef]
16. Khantuleva, T.A. Thermodynamic evolution far from equilibrium. In *AIP Conference Proceedings*; AIP Publishing LLC: Melville, NY, USA, 2018; Volume 1959, pp. 100003-1–100003-4. [CrossRef]
17. Khantuleva, T.A. *Mathematical Modeling of Shock-Wave Processes in Condensed Matter. (Ser. Shock Wave and High Pressure Phenomena)*; Springer Nature Pte Ltd.: Singapore, 2022; p. 336. [CrossRef]
18. Hintze, J.O. *Turbulence*; Mc. Graw Hill Inc.: New York, NY, USA, 1962; p. 546.
19. Camussi, R.; Guj, G.; Ragni, A. Wall pressure fluctuations induced by turbulent boundary layers over surface discontinuities. *J. Sound Vib.* **2006**, *294*, 177–204. [CrossRef]
20. Landau, L.D.; Lifshitz, E.M. *Fluid Mech: Course of Theoretical Physics*; Elsevier: Amsterdam, The Netherlands, 1987; Volume 6.
21. Pope, S.B. *Turbulent Flows*; Cambridge University Press: Cambridge, UK, 2000.
22. Piquet, J. *Turbulent Flows*; Revised 2nd Printing; Springer: Berlin, Germany, 2001.
23. Faisst, H.; Eckhardt, B. Sensitive dependence on initial conditions in transition to turbulemce in pipe flow. *J. Fluid Mech.* **2004**, *594*, 343–352. [CrossRef]
24. Liu, C.; Yan, Y.; Lu, P. Physics of turbulence generation and sustenance in a boundary layer. *Comput. Fluids* **2004**, *102*, 353–384. [CrossRef]
25. Yano, K.; Horie, Y. Discrete element modeling of shock compression of polycrystalline copper. *Phys. Rev. B* **1999**, *59*, 13672–13680. [CrossRef]
26. Richardson, J. The hydrodynamic equations of a one-component system derived from nonequilibrium statistical mechanics. *J. Math. Anal. Appl.* **1960**, *1*, 12–60. [CrossRef]
27. Chung, C.H.; Yip, S. Generalized hydrodynamics and time correlation functions. *Phys. Rev.* **1965**, *182*, 323–338. [CrossRef]
28. Piccirelli, R. Theory of the dynamics of simple fluid for large spatial gradients and long memory. *Phys. Rev.* **1968**, *175*, 77–98.
29. Ailavadi, N.; Rahman, A.; Zwanzig, R. Generalized hydrodynamics and analysis of current correlation functions. *Phys. Rev.* **1971**, *4*, 1616–1625. [CrossRef]
30. Edelen, D.G. *Nonlocal Field Theories in Continuum Physics*; Academic Press Inc.: Cambridge, MA, USA, 1976; p. 4.
31. Zubarev, D.N. *Non-Equilibrium Statistical Thermodynamics*; Springer: Berlin/Heidelberg, Germany, 1974.
32. Zubarev, D.N.; Tischenko, S.V. Nonlocal hydrodynamics with memory. *Physics* **1972**, *59*, 285–304. [CrossRef]
33. Kuzemsky, A.L. Theory of transport processes and the method of the nonequilibrium statistical operator. *Int. J. Mod. Phys. B* **1972**, *21*, 2821–2919. [CrossRef]
34. Fradkov, A.L. *Cybernetical Physics: From Control of Chaos to Quantum Control*; Springer: Berlin, Germany, 2007.
35. Fradkov, A.L. Horizons of cybernetical physics. *Philos. Trans. R. Soc. A Math. Phys. Eng. Sci.* **2017**, *375*, 20160223. [CrossRef]
36. Khantuleva, T.A.; Kats, V.M. Quantum Effects on the Mesoscale. *Particles* **2020**, *3*, 562–575. [CrossRef]
37. Klimontovich, Y.L. Entropy and information of open systems. *Phys. Usp.* **1999**, *42*, 375–384. [CrossRef]
38. Klimontovich, Y.L. Relative ordering criteria in open system. *Phys. Usp.* **1996**, *39*, 1169–1179. [CrossRef]
39. Klimontovich, Y.L. *Turbul. Motion Chaos Struct*; Nauka: Moscow, Russia, 1990. (In Russian)
40. Aero, E.L.; Bulygin, A.I.; Kuvshinskiy, E.I. Asymmetric hydrodynamics. *Prikl. Mat. I Mekhanika* **1965**, *29*, 297–308. (In Russian)
41. Meshcheryakov, Y.I.; Khantuleva, T.A. Nonequilibrium Processes in Condensed Media. Part 1. Experimental Studies in Light of Nonlocal Transport Theory. *Phys. Mesomech.* **2015**, *18*, 228–243. [CrossRef]
42. Nicolis, G.; Prigogine, I. Self-Organization in Nonequilibrium Systems. In *Dissipative Structure to Order through Fluctuations*; Wiley: New York, NY, USA, 1977; p. 320.
43. Glansdorff, P.; Prigogine, I. *Thermodynamic Theory of Structure, Stability and Fluctuations*; Wiley Interscience: Hoboken, NJ, USA, 1972.
44. Ivanov, M.G. *How to Understand Quantum Mechanics*; R&C Dynamics: Moskow-Izhevsk, Russia, 2012. (In Russian)

45. Gilman, J.J. Response of condensed matter to impact. In *High Pressure Shock Compression of Solids VI. Old Paradigms and New Challenges*; Horie, Y.-Y., Davison, L., Thadhani, N.N., Eds.; Springer: Berlin/Heidelberg, Germany, 2003; pp. 279–296.
46. Meshcheryakov, Y.I.; Divakov, A.K.; Zhigacheva, N.I.; Barakhtin, B.K. Regimes of interscale momentum exchange in shock deformed solids. *Int. J. Impact Eng.* **2013**, *57*, 99–107. [CrossRef]